

## Electric field and power flow predictions for ICRF Antennas with TOPICA

B. Van Compernelle<sup>1</sup>, R. Koch<sup>1</sup>, P.U. Lamalle<sup>1</sup>, F. Louche<sup>1</sup>, R. Maggiore<sup>2</sup>,  
V. Lancellotti<sup>2</sup>, D. Milanese<sup>2</sup>

<sup>1</sup>Laboratory for Plasma Physics - Association 'Euratom-Belgian State'  
Ecole Royale Militaire - Koninklijke Militaire School, B-1000 Brussels, Belgium\*

<sup>2</sup>Politecnico di Torino, Dipartimento di Elettronica, Torino, Italy

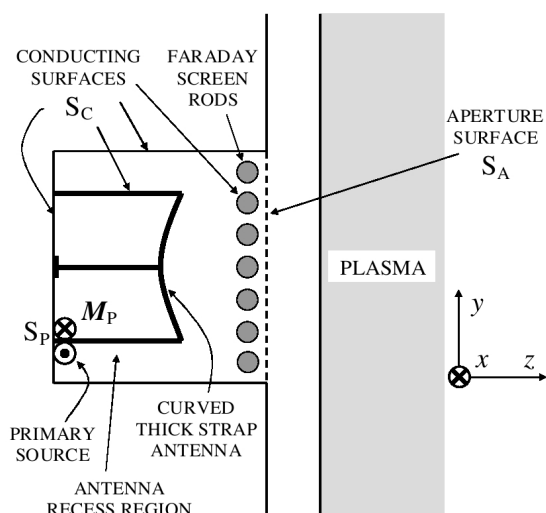
\* Partner in the Trilateral Euregio Cluster (TEC).

### Introduction

TOPICA [1] is presently the only code which combines accurate 3D modelling of ICRF antennas with a realistic 1D plasma model. The natural outputs of TOPICA are the currents on the conductors and the admittance matrix of the antenna. Although these parameters are sufficient to evaluate new antenna designs and to design matching circuits for them, the need to also investigate their vulnerability to sheath effects necessitates the explicit calculation of the radiated fields. A post-processing module has been developed which calculates these fields, both in the vacuum gap between the antenna aperture and the plasma edge, and in the plasma itself.

### Radiated Fields

TOPICA calculates the electric and magnetic currents on all surfaces of a 3D antenna, located in vacuum and radiating towards a 1D plasma. The knowledge of the magnetic currents on the aperture of the antenna and the knowledge of the surface impedance matrix at the plasma edge, is sufficient to calculate the radiated fields in the vacuum gap between the aperture and the plasma. The surface impedance matrix relates the transverse electric and magnetic fields at the plasma edge, and is provided by the 1D plasma code FELICE [2]. FELICE uses the FLR equations (Swanson-Colestock-Kashuba approximation and assuming single pass absorption) to solve for the electric field  $\mathbf{E}(k_x, k_y, z)$  ( $z$  is the radial direction), for the two inde-



pendent polarizations of the incident field; one polarization with  $B_y = 0$  and one with  $B_x = 0$ . The solution at the plasma edge determines the plasma surface impedance matrix  $Z_P$ , defined by  $\mathbf{E}_t = Z_P \cdot (\mathbf{H}_t \times \hat{z})$ .

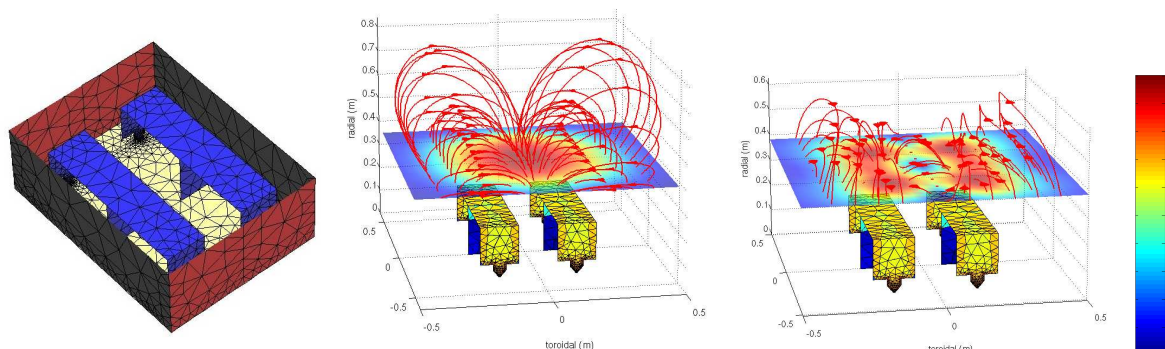
Maxwell's equations can be written in terms of transverse and radial field components. In vacuum, Maxwell's equations for the transverse field components, in cylindrical  $(k_t, \sigma, k_z)$  basis, become

$$\begin{aligned} -\frac{d\mathbf{E}_t}{dz} &= jk_z \overleftrightarrow{Z}_\infty \cdot (\mathbf{H}_t \times \hat{z}) \\ -\frac{d\mathbf{H}_t \times \hat{z}}{dz} &= jk_z \overleftrightarrow{Y}_\infty \cdot \mathbf{E}_t \end{aligned}$$

with  $\overleftrightarrow{Z}_\infty(\mathbf{k}_t) = \overleftrightarrow{Y}_\infty^{-1}(\mathbf{k}_t) = \frac{Z_0 k_z}{k_0} \hat{k}_t \hat{k}_t + \frac{Z_0 k_0}{k_z} \hat{\sigma} \hat{\sigma}$ ,  $k_z = (k_0^2 - k_t^2)^{1/2}$ . These equations combined with the fields  $\mathbf{E}_t$  at the antenna aperture (known outputs of TOPICA calculation), and the surface impedance matrix at the plasma edge, allow for the calculation of all the fields in the vacuum gap. The FELICE code was adapted to output the electromagnetic fields at user specified radial locations for both incoming polarizations. The input spectrum at the plasma edge is now known from the calculation of the fields in the vacuum gap, and is used to calculate the fields in the plasma radiated by the antenna.

### Vacuum Loading

As a reference case the doublestrap antenna depicted below is simulated radiating into vacuum, in dipole phasing (current on both straps 180° out of phase). The pictures below show field lines of magnetic (middle) and electric (right) fields, as well as the magnitude of the fields in a plane above the antenna aperture. Also shown is the amplitude of the strap currents (log scale normalized to [0,1]).

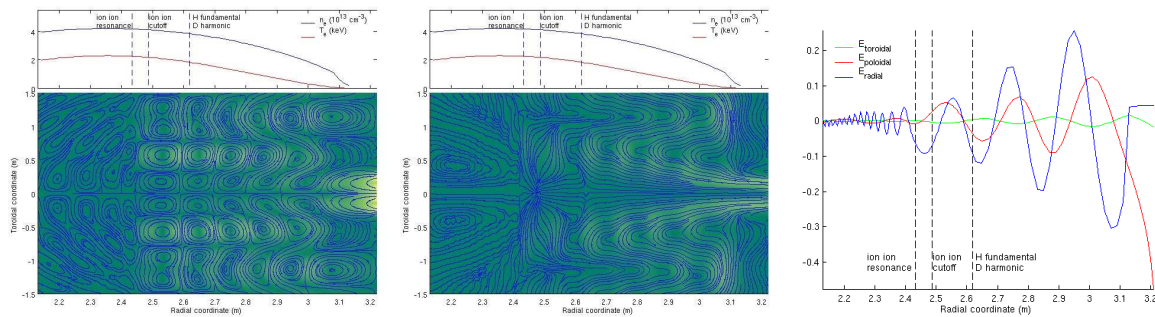


### Plasma Loading

The same doublestrap antenna now radiates into a D plasma, with 10% H minority. The central density is  $4.2 \cdot 10^{13} \text{ cm}^{-3}$ , with a vacuum gap of 9 cm between aperture and plasma edge

and a central electron temperature of 2.3 keV (see profiles in plots below). The magnetic field at center is 2.35 T and has a  $7^\circ$  tilt.

The figures below show contour plots of magnetic field amplitude (left) and Poynting flux magnitude (middle) in colors (light green: high amplitude, dark green: low amplitude), overlaid with the respective field lines. The observation plane is a poloidal cut at  $y = 0$  m. The top of the figures shows  $T_e$  and  $n_e$  radial profiles near the antenna.



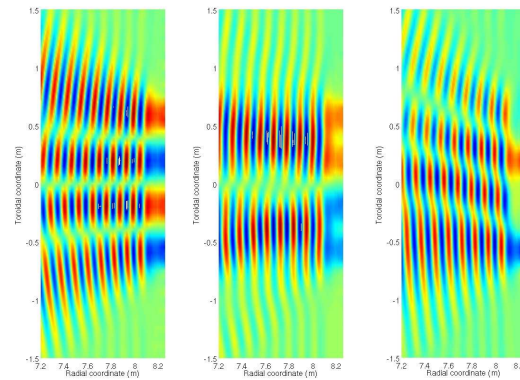
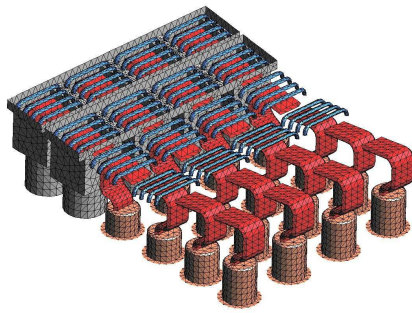
A large part of the power is reflected at the ion-ion hybrid cut-off, as is clear from the Poynting flux picture. The wave is caught between two cut-offs, and undergoes multiple reflections at the ion-ion hybrid cut-off and at the low density cut-off. The large reflected power is also the cause of the standing wave pattern in the magnetic field picture.

Part of the power tunnels through the ion-ion evanescence zone to the hybrid resonance and undergoes mode conversion to an ion hybrid wave. This is also obvious from the picture on the right, which displays the radial profile of the electric field components in front of one of the straps. Past the resonance the fast wave mode converts into a short wavelength electrostatic wave.

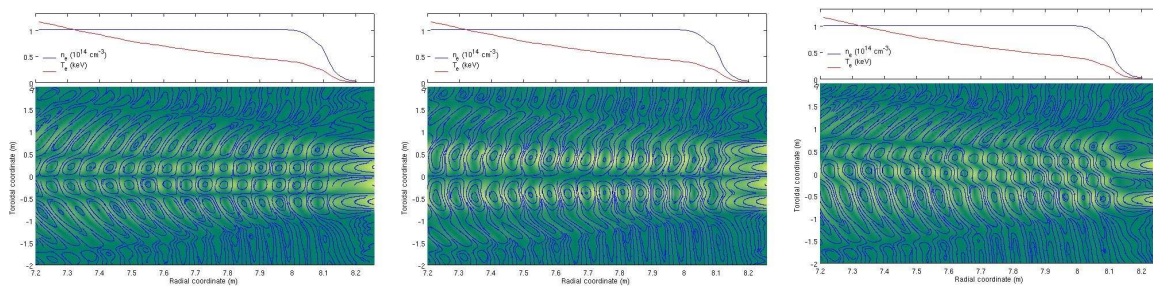
## ITER Antenna

The post-processing code was also used to visualize the fields radiated by the proposed design for the ITER antenna [3]. Results were obtained for 3 different toroidal phasings, namely  $(0, \pi, 0, \pi)$  phasing,  $(0, 0, \pi, \pi)$  phasing and current drive  $(0, \pi/2, \pi, 3\pi/2)$  phasing. The current on the straps is in phase poloidally. The plasma is a mixture of 50% D, 50% T, with a scrape-off layer of 15 cm, a central electron temperature of 2.4 keV, a central density of  $1.02 \cdot 10^{14} \text{ cm}^{-3}$ , a central magnetic field of 6.2 T, and a magnetic field tilt angle of  $15^\circ$ .

A CAD model of the antenna is displayed below, with the Faraday screens and antenna enclosure removed on several straps. On the right, the toroidal magnetic field component  $H_x$  is plotted in a poloidal cut at  $y = .15$  m, for the three phasings (from left to right:  $(0, \pi, 0, \pi)$ ,  $(0, 0, \pi, \pi)$  and  $(0, \pi/2, \pi, 3\pi/2)$ ).



The magnetic field amplitude (in color) and the field lines of the magnetic field are plotted below for the same three phasings. These are poloidal cuts at  $y = .15$  m.



## Conclusions

A post-processing code has been developed for the TOPICA code. The code explicitly calculates the 3D electric and magnetic fields radiated by ICRH antennas. Examples with simple antennas radiating towards vacuum and towards a plasma, and examples with complex antennas have shown that these 3D fields can provide a better understanding of the behavior of ICRH antennas. The calculated fields can also be used to investigate possible detrimental sheath effects, and anticipate weak spots in the design in this respect.

## Acknowledgments

## References

- [1] V. Lancellotti, D. Milanesio, R. Maggiara, G. Vecchi and V. Kyrlytsya, *TOPICA: an accurate and efficient numerical tool for analysis and design of ICRF antennas*, Nuclear Fusion, **46**, S476-S499 (2006)
- [2] M. Brambilla, *Evaluation of the surface admittance matrix of a plasma in the finite larmor radius approximation*, Nuclear Fusion, **35**, 1265-1280 (1995)
- [3] P.U. Lamalle et al, *Status of the ITER ICRF system design - 'Externally Matched' approach*, 17th RF Topical Conference (2007)